# The A34R Glycoprotein Gene Is Required for Induction of Specialized Actin-Containing Microvilli and Efficient Cell-to-Cell Transmission of Vaccinia Virus

ELIZABETH J. WOLFFE, EHUD KATZ,† ANDREA WEISBERG, AND BERNARD MOSS*

*Laboratory of Viral Diseases, National Institute of Allergy and Infectious Diseases, National Institutes of Health, Bethesda, MD 20892-0445*

**The mechanisms allowing vaccinia virus to spread from cell to cell are incompletely understood. The A34R gene of vaccinia virus encodes a glycoprotein that is localized in the outer membranes of extracellular virions. The small-plaque phenotype of an A34R deletion mutant was similar to that of mutants with deletions in other envelope genes that fail to produce extracellular vaccinia virions. Transmission electron microscopy, however, revealed that the A34R mutant produced numerous extracellular particles that were labeled with antibodies to other outer-envelope proteins and with protein A-colloidal gold. Fluorescence and scanning electron microscopy indicated that expression of the A34R protein was necessary for detection of vaccinia virus-induced actin tails, which provide motility to the intracellular enveloped form of vaccinia virus, and of virus-tipped specialized microvilli that project from the cell. The ability of vaccinia virus-infected cells to form syncytia after a brief exposure to a pH below 6, known as fusion from within, failed to occur in the absence of expression of the A34R protein; nevertheless, purified A34R⁻ virions were capable of mediating low-pH-induced fusion from without. The present study provides genetic and microscopic evidence for the involvement of a specific viral protein in the formation or stability of actin-containing microvilli and for a role of these structures in cell-to-cell spread rather than in formation of extracellular virions.**

The mechanisms allowing vaccinia virus to spread from cell to cell are incompletely understood. Vaccinia virus assembly occurs in the cytoplasm, resulting in the formation of several related intra- and extracellular particles (8, 27). Two forms of potentially infectious intracellular particles have been described: intracellular mature virions (IMV) with two membranes, acquired from the intermediate compartment between the endoplasmic reticulum and the Golgi network (37), and intracellular enveloped virions (IEV) with four membranes, derived from IMV that have been wrapped with trans-Golgi cisternae (19, 37). Extracellular infectious particles arise by fusion of the outer IEV membrane with the plasma membrane, resulting in particles with the double IMV membrane plus one remaining Golgi network-derived membrane. Extracellular particles adhering to the cell membrane are called cell-associated enveloped virions (CEV) and probably mediate direct cell-to-cell spread (3); those released are called extracellular enveloped virions (EEV) and allow long-range spread (29). With some virus strains and cell types, EEV may also arise by budding of IMV through the plasma membrane (40, 41).

Recent studies suggest that the spread of vaccinia virus is not a passive process but is driven by the projection of virus-tipped actin-containing microvilli to neighboring uninfected cells (6). Numerous thickened microvilli, many tipped by a wrapped vaccinia virus particle attached to an actin tail, are on the surfaces of infected cells (6, 17, 20, 25, 38). Virus particles that appear to be exiting through these microvilli were seen in high-voltage electron microscopic images (38). Inhibitor studies suggested that virus particle assembly is required for the induction of these actin-containing microvilli (16, 25), and genetic studies indicated that IEV are needed (2). Cudmore et al. (6, 7) recently demonstrated that the actin tails propel the IEV within the cytoplasm at a speed of nearly 3 μm/min and that microvilli form when the particles reach the periphery of the cell. A vaccinia virus-tipped actin projection was shown to extend from an infected cell to an uninfected one, consistent with a role for actin in virus spread (6). Evidence that these protrusions play a significant role in transmission, however, has not yet been obtained.

The viral proteins involved in actin tail formation have not been identified. The homology of the A42R protein to profilin suggested such a role; however, deletion of the gene had no effect on formation of actin tails or thick microvilli (1). An 11-kDa phosphorylated protein is exposed on the surface of IMV particles and interacts with actin-containing cytoskeletal elements (18). A phosphorylated protein of this size is encoded by the F17R gene (45). However, recent data do not support a role for the F17R protein in actin tail formation (32). Since the actin tails propel IEV but not IMV, it would seem likely that an actin attachment protein is on the cytoplasmic surface of IEV.

Comparisons of IMV and EEV revealed that there are several membrane proteins specific for the latter (29, 30) (and presumably also for IEV and CEV since they also have the extra wrapping membrane). A major nonglycosylated EEV protein is encoded by the F13L gene (21, 34), and five glycosylated EEV proteins are encoded by the A33R (33), A34R (10), A36R (28), A56R (5, 36), and B5R (13, 22) genes. The latter contains Golgi membrane and EEV targeting signals (23). The consequences of deleting or repressing expression of each of these genes, with the exception of A33R, have been reported. None of the EEV proteins are required for formation of infectious IMV. Nevertheless, a small-plaque phenotype was observed when expression of the F13L (2), A34R

* Corresponding author. Mailing address: Laboratory of Viral Diseases, NIAID, NIH, Building 4, Room 229, 4 Center Dr., MSC 0445, Bethesda, MD 20892-0445. Phone: (301) 496-9869. Fax: (301) 480-1147. E-mail: bmoss@nih.gov.
† Permanent address: Department of Virology, Hebrew University-Hadassah Medical School, Jerusalem 91120, Israel.
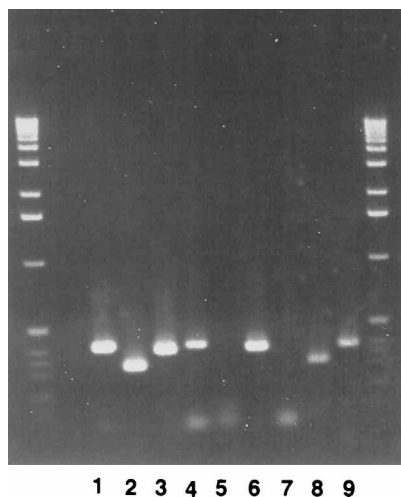
FIG. 1. Genotypic characterization of the A34R⁻ mutant. The DNA present in lysates of cells infected with wild-type vaccinia virus (lanes 1 to 3), vSAD9 (lanes 4 to 6), and vA34R⁻ (v41) (lanes 7 to 9) were analyzed by PCR with primers for the A34R (lanes 1, 4, and 7), TK (lanes 2, 5, and 8), and A43R (lanes 3, 6, and 9) genes. The latter provided a positive control for a nonmutated viral DNA region whose size was similar to that of the A34R PCR product. The PCR products were analyzed by agarose gel electrophoresis with lambda DNA HindIII digests at the extreme left and right lanes.

(10), A36R (28), or B5R (14, 42) gene was prevented, indicating that IMV are insufficient to mediate efficient cell-to-cell spread. A neutral-pH syncytial phenotype occurred when A56R was mutated (35), and a point mutation within the lectin homology domain of the A34R gene affected the release of CEV and determined whether plaques formed in liquid medium were round or had an extended comet shape indicative of long-range virus spread (4).

In principle, a small-plaque phenotype could arise from a variety of defects in virus assembly or spread. Thus, F13L (2), B5R (14, 42) and A36R (28) mutants produce reduced amounts of extracellular virus. Electron microscopic examination of cells infected with F13L (2) or B5R (14, 42) mutants indicated that wrapping of IMV to form IEV was blocked. Electron microscopic studies of a small-plaque-forming A34R mutant indicated a similar defect in EEV formation (10), but a follow-up biochemical analysis suggested that EEV of low infectivity were formed (26). These findings suggested a novel phenotype for the A34R mutant, making further investigation of the role of this viral gene in morphogenesis and virus spread important.

In the present study, the small-plaque phenotype of an A34R deletion mutant was confirmed; nevertheless, both IEV and EEV were visualized by electron microscopy of infected cells. Novel findings of impaired formation of actin tails, thickened microvilli, and low-pH-induced syncytia support a role for actin-containing microvilli in virus spread rather than EEV formation.

## MATERIALS AND METHODS

**Viruses and cells.** HeLa S3 (ATCC CCL 2.2), BS-C-1 (ATCC CCL 26), CV-1 (ATCC CCL 70), and RK$_{13}$ (ATCC CCL 37) cells were grown in E-MEM (Quality Biologicals, Gaithersburg, Md.) supplemented with 10% fetal calf serum. Vaccinia virus strains WR (ATCC VR-1354) and IHD-J (derived from ATCC VR-156) and recombinant viruses prepared from them were propagated as described previously (11).

An A34R⁻ recombinant vaccinia virus (vA34R⁻ [code name, v41]) was derived as follows. CV-1 cells were infected with vSAD9 (10) and transfected with a plasmid containing the HindIII J fragment of vaccinia virus strain WR, and

thymidine kinase (TK)-positive virions were plaque purified as described previously (12).

**Plaque formation.** BS-C-1 monolayers in six-well dishes (Costar Corp., Cambridge, Mass.) were inoculated with 0.2 ml of a diluted virus stock. After 1 h at 37°C, an overlay medium with 0.7% low-melting-point agarose (Life Technologies Inc., Grand Island, N.Y.) with or without 50 mM isopropyl-β-D-thiogalactopyranoside (IPTG; Gold Biotechnology Inc., St. Louis, Mo.) was added. After 3 days, the cells were fixed with 20% formaldehyde in phosphate-buffered saline (PBS) and stained with crystal violet (0.1% in 0.1 M citric acid).

**PCR.** Infected-cell lysates were clarified by centrifugation and incubated with an equal volume of Nonidet P-40 (0.9%)–Tween 20 (0.9%) at room temperature for 5 min. Proteinase K (250 μg/ml) was then added, and the incubation was continued for 1 h at 37°C. The mixture was then heated at 94°C for 14 min, and the PCR was initiated by addition of 30 pmol of each oligonucleotide primer. The DNA products formed after 35 cycles of 1 min at 94°C, 1 min at 55°C, and 2 min at 72°C were analyzed by electrophoresis in a 1.4% agarose gel with a HindIII digest of lambda DNA as the standard.

**Fluorescence microscopy.** Fluorescence microscopy was performed as previously described (44). Briefly, infected HeLa cell monolayers on coverslips were washed with PBS, fixed in 3% paraformaldehyde, and permeabilized with 0.05% saponin (Calbiochem, San Diego, Calif.). Actin filaments were visualized with fluorescein isothiocyanate (FITC)-conjugated phalloidin (Molecular Probes, Eugene, Oreg.). The infection status of the cells was checked by incubating them first with a rabbit polyclonal antiserum that recognizes the B5R and F13L proteins (16) and then with rhodamine-conjugated swine anti-rabbit antiserum (Dako Corporation, Carpinteria, Calif.).

**Electron microscopy.** For transmission electron microscopy, infected RK$_{13}$ cells were fixed and prepared for embedding in EMbed-812 (Electron Microscopy Sciences, Fort Washington, Pa.) or prepared for cryoimmunoelectron microscopy as previously described (43). Epon-embedded samples were sectioned and viewed directly. Thawed cryosections were incubated first with a rabbit polyclonal antiserum against the B5R and F13L proteins (16) and then with 10-nm-diameter gold particles conjugated to protein A (Department of Cell Biology, Utrecht University School of Medicine, Utrecht, The Netherlands) as described previously (43). Samples were viewed with a Philips CM 100 electron microscope.

For scanning electron microscopy, HeLa cells grown on coverslips and infected (or not) were immersed in a graded series of fixatives up to a final concentration of 2% glutaraldehyde in 0.1 M sodium cacodylate (pH 7.4). Coverslips were washed in cacodylate buffer, and the cells were postfixed with 2% osmium tetroxide on ice. After fixation, the samples were dehydrated in a graded series of acetone and finally treated with hexamethyldisilazane (Electron Microscopy
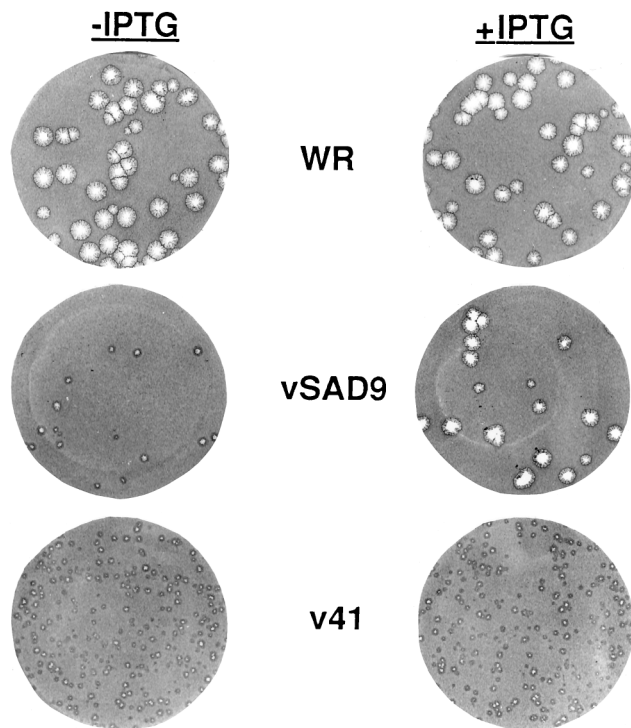


FIG. 2. Plaque phenotypes of A34R mutant vaccinia viruses. Plaques that formed after 3 days with an agar overlay in the absence (−) or presence (+) of IPTG were stained with crystal violet and photographed.
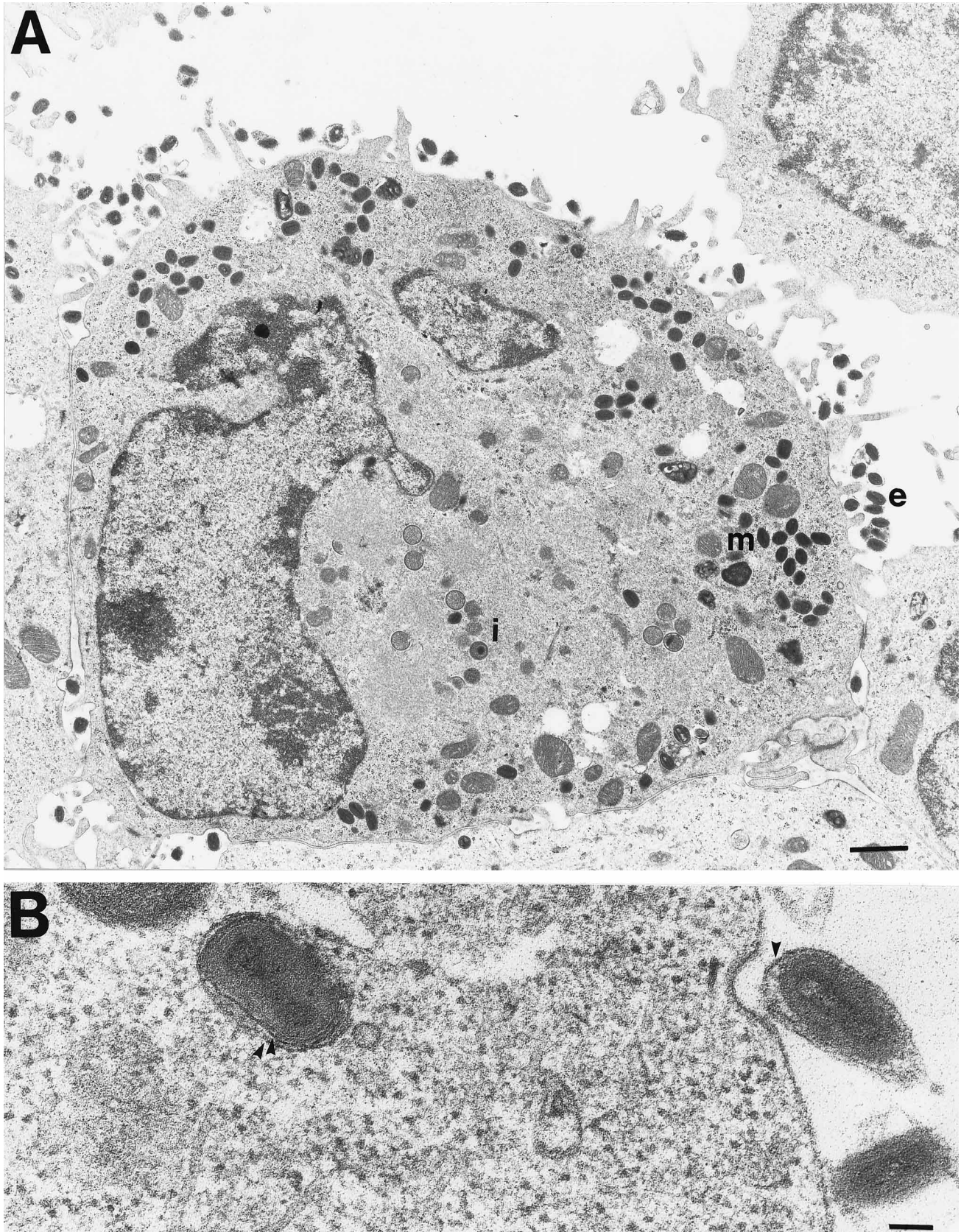
FIG. 3. Transmission electron microscopy of cells infected with vA34R⁻. (A) Section through an entire cell, with examples of immature virus (i), IMV (m), and EEV (e). Bar, 1.0 μm. (B) View of an IEV and an EEV with double and single Golgi-derived membranes, respectively, indicated by arrowheads. Bar, 0.1 μm.
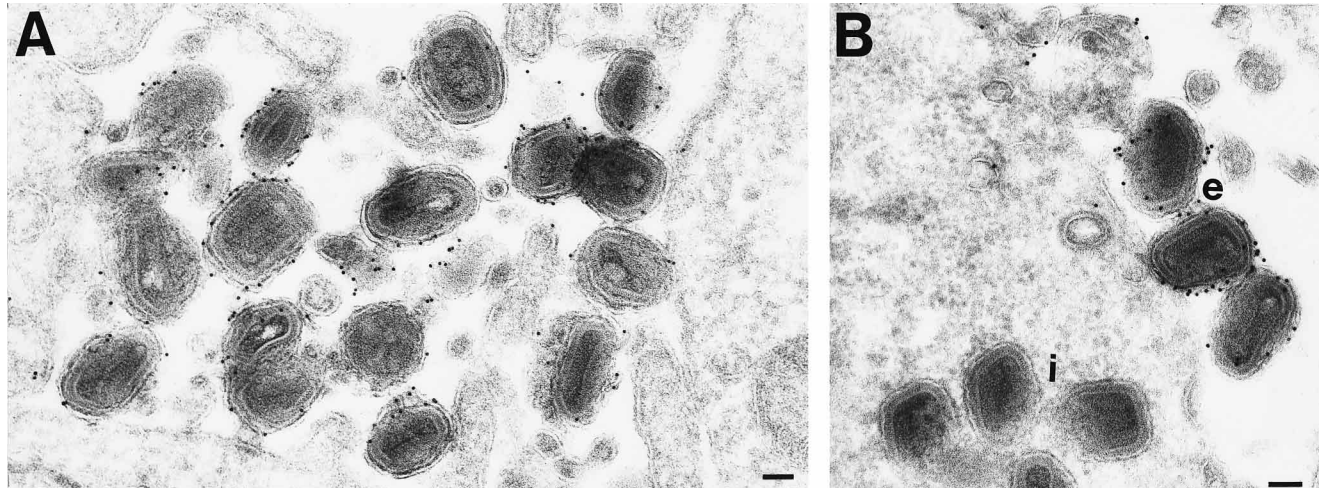
FIG. 4. Immunogold labeling of A34R⁻ extracellular particles. Thawed cryosections of cells infected with vA34R⁻ were immunogold labeled with a rabbit antiserum that reacted with the F13L and B5R EEV proteins. (A) Numerous EEV are shown. Bar, 0.1 μm. (B) Unlabeled intracellular IMV (i) and labeled extracellular (e) particles are shown. Bar, 0.1 μm.

Sciences). The coverslips were air dried, mounted on stubs, and coated with silver. Samples were examined with a Jeol JSM 35 CF microscope at an accelerating voltage of 15 kV.

**Low-pH-induced syncytium formation.** Fusion from within was carried out essentially as described previously (2, 9). Briefly, BS-C-1 cells were infected with 10 PFU of wild-type or recombinant virus per cell. At 20 h after infection, the cells were washed with PBS and treated for 2 min at 37°C with low-pH fusion buffer [PBS with 10 mM 2-(N-morpholino)ethanesulfonic acid (MES) and 10 mM HEPES at pH 5.5] or with a neutral-pH nonfusion buffer containing the same components at pH 7.4. The low-pH or neutral buffer was replaced with E-MEM supplemented with 3% fetal calf serum, and the cells were incubated at 37°C for 2.5 h. The cells were fixed with 1% glutaraldehyde in PBS and stained with crystal violet (0.1% in 0.1 M citric acid).

Fusion from without was done essentially as described previously (15). Monolayers of BS-C-1 cells were kept on ice for 15 min and then infected with purified virus (2,000 virions per cell) in the presence of cycloheximide (300 μg/ml) for 1 h. Unbound virus was removed with the medium, and E-MEM supplemented with 2% fetal calf serum containing cycloheximide was added. After 30 min at 0°C, the medium was replaced with either low-pH fusion buffer or neutral-pH nonfusion buffer, and the incubation was continued for 3 h at 37°C. The cells were then fixed with methanol-acetone and stained with crystal violet.

## RESULTS

**Construction and plaque phenotype of vA34R⁻.** Recombinant vaccinia virus vSAD9 has an IPTG-inducible copy of the A34R gene in the TK locus and a deletion of nearly the entire natural A34R gene (10). We deleted the inducible gene copy from vSAD9 by homologous recombination with a vaccinia virus DNA fragment containing an intact TK gene to produce a true null mutant. The TK⁺ virus, named vA34R⁻ (v41), was isolated by using TK⁻143 cells and selection medium. The TK⁺ A34R⁻ genotype of vA34R⁻ was confirmed by PCR with primers specific for the two viral genes and comparisons with the TK⁺ A34R⁺ genome of wild-type vaccinia virus and with the TK⁻ A34R⁺ genome of vSAD9 (Fig. 1).

The plaque phenotypes of vaccinia virus strains WR, vSAD9, and vA34R⁻ (v41) were examined with and without the presence of IPTG in the agar overlay (Fig. 2). The plaque size of standard WR strain virus was unaffected by IPTG. As previously shown (10), vSAD9 plaques were small in the absence of IPTG and of normal size in the presence of this inducer. In contrast, vA34R⁻ plaques were unaffected by this inducer and slightly smaller than those of vSAD9. The latter results are similar to those reported for an independently derived A34R deletion mutant (26) and indicate a defect in virus spread.

Despite the small size of vA34R⁻ plaques, the titers of virus

stocks obtained by lysis of infected cells were similar to those of wild-type vaccinia virus WR, suggesting that there was no defect in the production or infectivity of IMV (data not shown). The titer of virus was severalfold higher in the medium of vA34R⁻-infected cells than in that of WR-infected cells after the released virus was frozen and thawed (data not shown), consistent with results obtained by McIntosh and Smith (26) with CsCl-purified EEV.

**Transmission electron microscopy.** RK₁₃ cells infected with vA34R⁻ were examined by transmission electron microscopy. A view of a section through an entire cell is shown in Fig. 3A. Immature viral forms are evident in the central region, and mature particles can be seen in the periphery. Significantly, numerous virus particles appear external to the cell membrane, although some of these could be connected through cytoplasmic protrusions that lie above or below the plane of the section. The appearance of cells infected with wild-type virus was similar, and therefore an image of them is not shown here.

An example of an IEV with a wrapping membrane and an EEV that appears to have been just released from a cell infected with vA34R⁻ are shown under high magnification in Fig. 3B. The concave shape and increased density of the adjacent plasma membrane could represent either the fused outer IEV membrane or a clathrin-coated pit (Fig. 3B). IEV are frequently found in clusters and in only some cell sections, making them difficult to quantitate. However, there seemed to be fewer clusters of IEV in cells infected with vA34R⁻ than in cells infected with wild-type virus.

To directly demonstrate that vA34R⁻ particles contained EEV membranes, thawed cryosections of HeLa cells infected with mutant virus were incubated with antibody to the F13L and B5R EEV proteins and examined by electron microscopy. Essentially all extracellular virus particles were immunogold labeled (Fig. 4). In contrast, IMV were unlabeled as expected (Fig. 4B).

**Phalloidin staining of actin filaments.** The possibility that the phenotype of some small-plaque mutants of vaccinia virus, e.g., A34R⁻, might be due to a defect in actin tail formation (39) was considered next. Vaccinia virus-induced actin tails have been visualized by fluorescence microscopy with antibody to actin (20) or with labeled phalloidin (1, 6). In uninfected HeLa cells, FITC-conjugated phalloidin stained long, slender
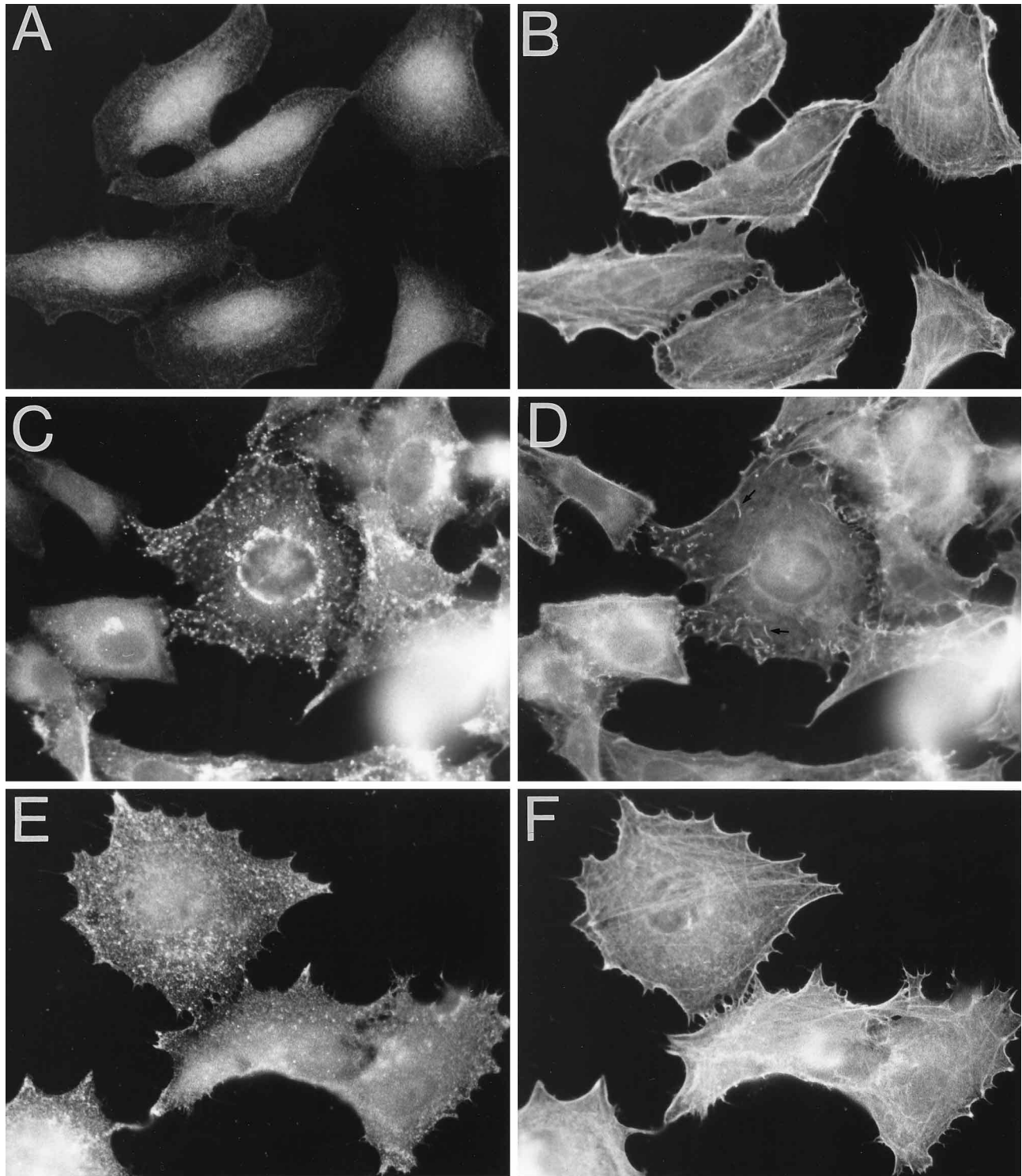
FIG. 5. Fluorescence microscopy of actin filaments and virus particles. Uninfected cells (A and B) and cells infected with wild-type virus (C and D), vA34R⁻ (E and F), vSAD9 without IPTG (G and H), and vSAD9 with IPTG (I and J) were stained with FITC-conjugated phalloidin and then incubated with rabbit antiserum to the EEV proteins encoded by F13R and B5R. The latter were visualized by using a rhodamine-conjugated swine anti-rabbit antibody. Photographs were taken using filters that recorded the antibody (A, C, E, G, and I) and phalloidin (B, D, F, H, and J) staining. Arrows point to examples of virus-induced actin tails.

stress fibers that constitute the actin cytoskeleton (Fig. 5B). After infection with standard vaccinia virus strain WR, numerous characteristic short, thick actin tails stained with phalloidin (Fig. 5D). The virus-induced actin tails are detectable in the

majority of infected cells and are easily distinguished from the normal actin filaments. In contrast, typical actin tails were not apparent in cells infected with vA34R⁻ (Fig. 5F) or with vSAD9 in the absence of IPTG (Fig. 5H). Nevertheless, they
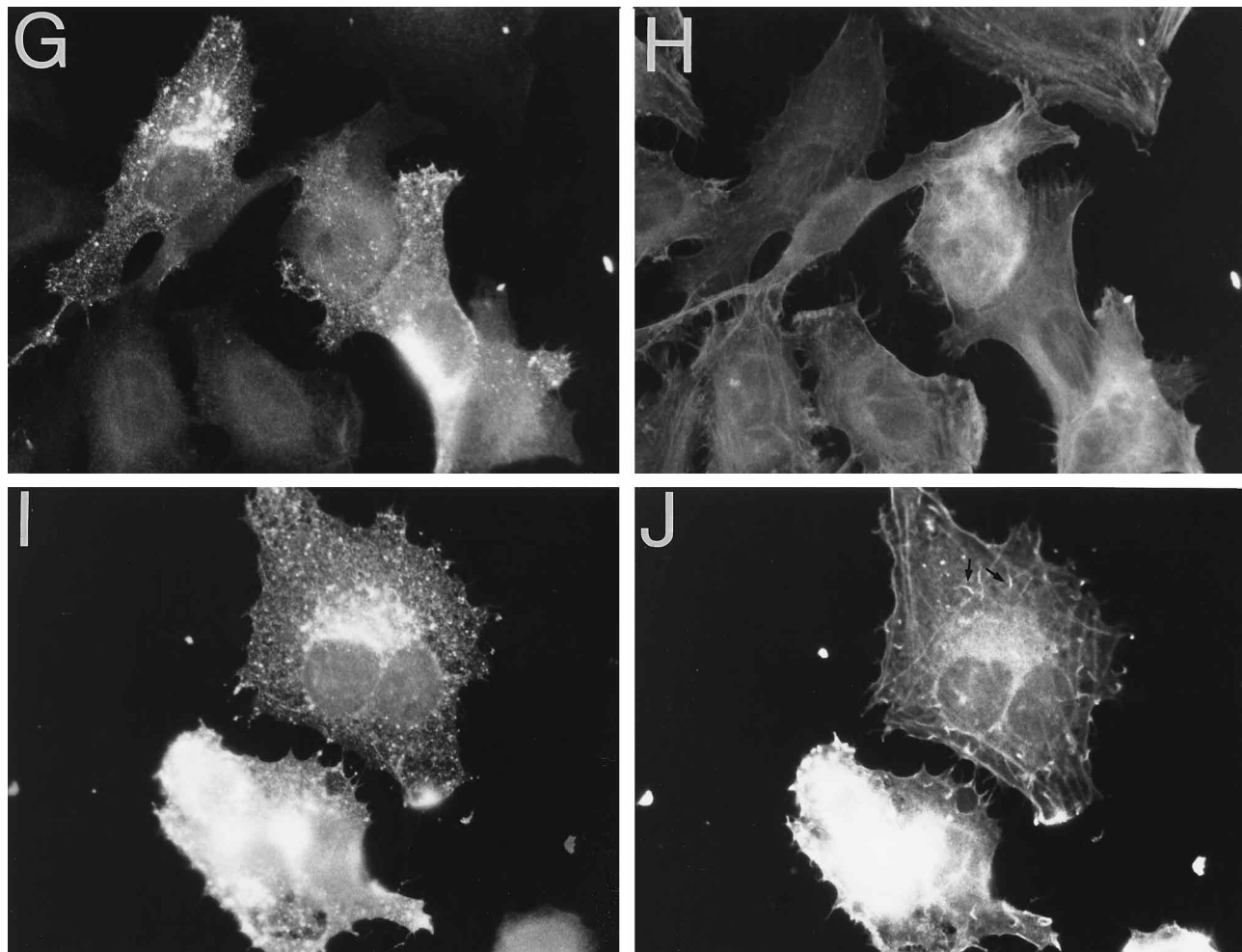
FIG. 5—*Continued.*

were abundant in cells infected with vSAD9 in the presence of IPTG (Fig. 5J).

To confirm that the cells were virus infected, the FITC-conjugated-phalloidin-stained cells were examined by incubating them first with antibody to the EEV proteins encoded by F13R and B5R and then with a rhodamine-conjugated secondary antibody. The antibody stained punctate regions, presumably representing wrapped virus particles and/or endosomes, in a similar manner in cells infected with wild-type virus (Fig. 5C), vA34R⁻ (Fig. 5E), vSAD9 (without [Fig. 5G] and with [Fig. 5I] IPTG), consistent with the results of the electron microscopic studies presented in the previous section. In most cells, antibody staining of a juxtanuclear mass that probably represents the Golgi network was also observed.

**Scanning electron microscopy.** Earlier studies suggested a relationship between vaccinia virus-induced actin bundle formation and specialized microvilli. We therefore examined the surfaces of wild-type- and recombinant-virus-infected HeLa cells by scanning electron microscopy. Slender microvilli were present on the surfaces of uninfected (Fig. 6A) and infected (Fig. 6B) cells. Thick, specialized microvilli of approximately 0.35 μm, the diameter of a virion, were also visualized on the surfaces of cells infected with wild-type virus (Fig. 6B). Examples of such thickened microvilli were not seen on uninfected cells or cells infected with vSAD9 in the absence of IPTG (Fig.

6C) or vA34R⁻ (Fig. 6E) but were clearly present when cells were infected with vSAD9 in the presence of IPTG (Fig. 6D). Thus, A34R expression was necessary for visualization of actin tails and specialized microvilli.

**Low-pH-induced syncytium formation.** Vaccinia virus-infected cells undergo fusion from within after a brief exposure to a pH below 6 (9, 15, 24), a phenomenon that may be related to events occurring during virus entry or spread. Gong et al. (15) provided evidence that fusion is mediated by a 14-kDa IMV protein. Cells infected with vaccinia virus mutants with deletions of F13R or B5R do not undergo acid-induced fusion, probably because the virions containing the 14-kDa protein are not presented on the cell surface when formation of extracellular virus is inhibited (2, 42).

vA34R⁻, unlike the F13R and B5R mutants, forms EEV. Based on previous studies, it might have been anticipated that vA34R⁻ virus would induce low-pH-mediated fusion. This was not the case, however. A control experiment demonstrated fusion in cells infected with wild-type vaccinia virus (Fig. 7D) but not in uninfected cells (data not shown) or cells infected with vA34R⁻ (Fig. 7E). The fusion-negative phenotype of vA34R⁻ virus was similar to that of cells infected with F13L⁻ virus (Fig. 7F). The cells in Fig. 7A to C are controls incubated only in neutral-pH buffers.

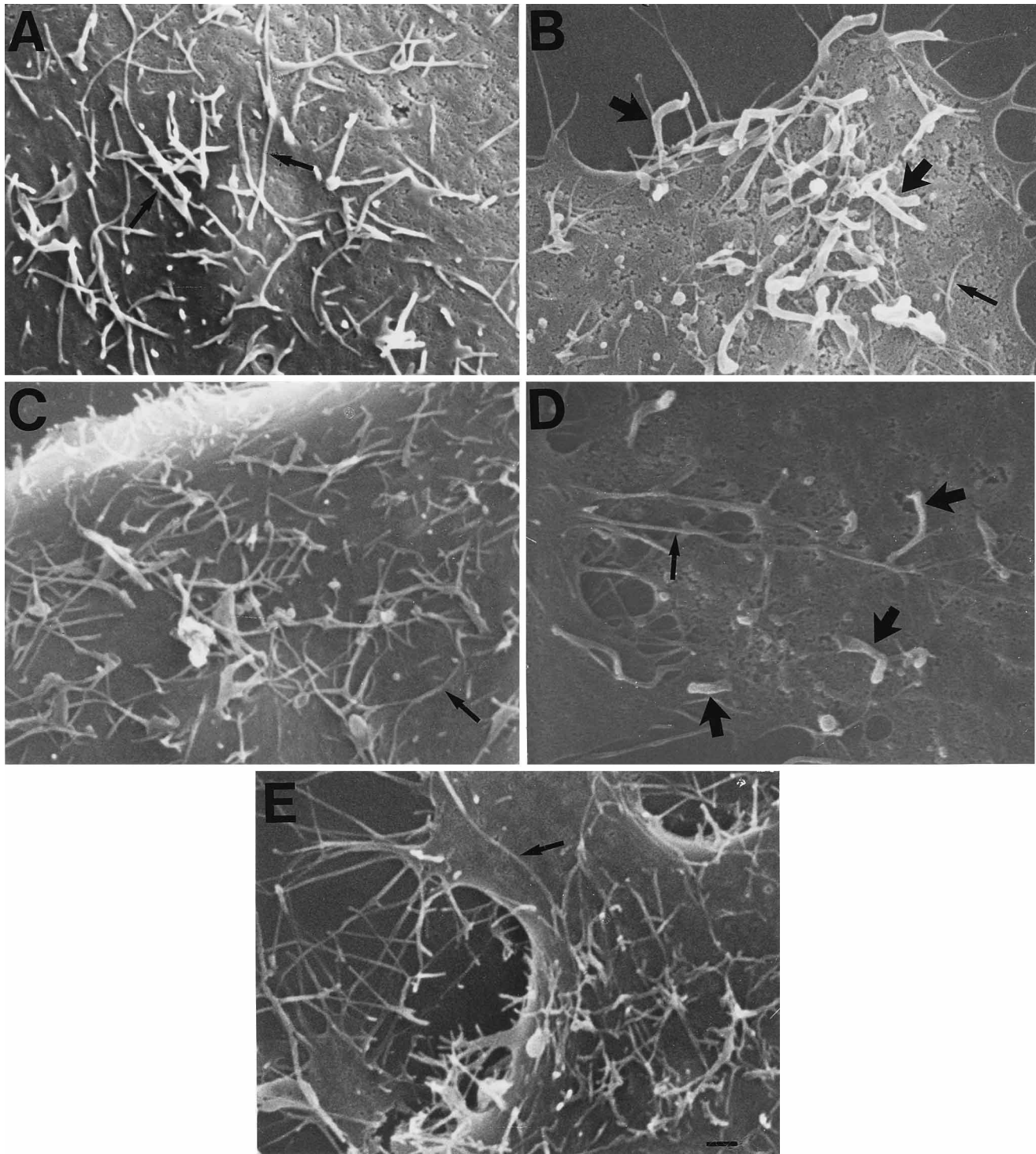To confirm that the defect in acid-induced fusion was due

FIG. 6. Scanning electron microscopy of the surfaces of uninfected cells (A) and of cells infected with wild-type WR virus (B), vSAD9 without IPTG (C), vSAD9 with IPTG (D), and vA34R⁻ (E). Thin and thick arrows point to examples of slender cellular and thick virus-induced microvilli, respectively. Bar, 1 μm.

solely to the absence of A34R gene expression, the experiment was repeated with vSAD9. In this case, fusion failed to occur in the absence of IPTG (Fig. 8C) and was inducer dependent (Fig. 8D). Cells in Fig. 8A and B are controls incubated only in neutral-pH buffers.

Fusion from without can be induced by briefly lowering the

pH after inoculating cells with purified intracellular vaccinia virus at a high multiplicity of infection in the presence of cycloheximide (15). This drug prevents the synthesis of viral proteins and the accompanying severe cytopathic effects of a normal infection. In Fig. 9, the clumped nuclei indicative of polykaryon formation are clearly seen for A34R and F13L
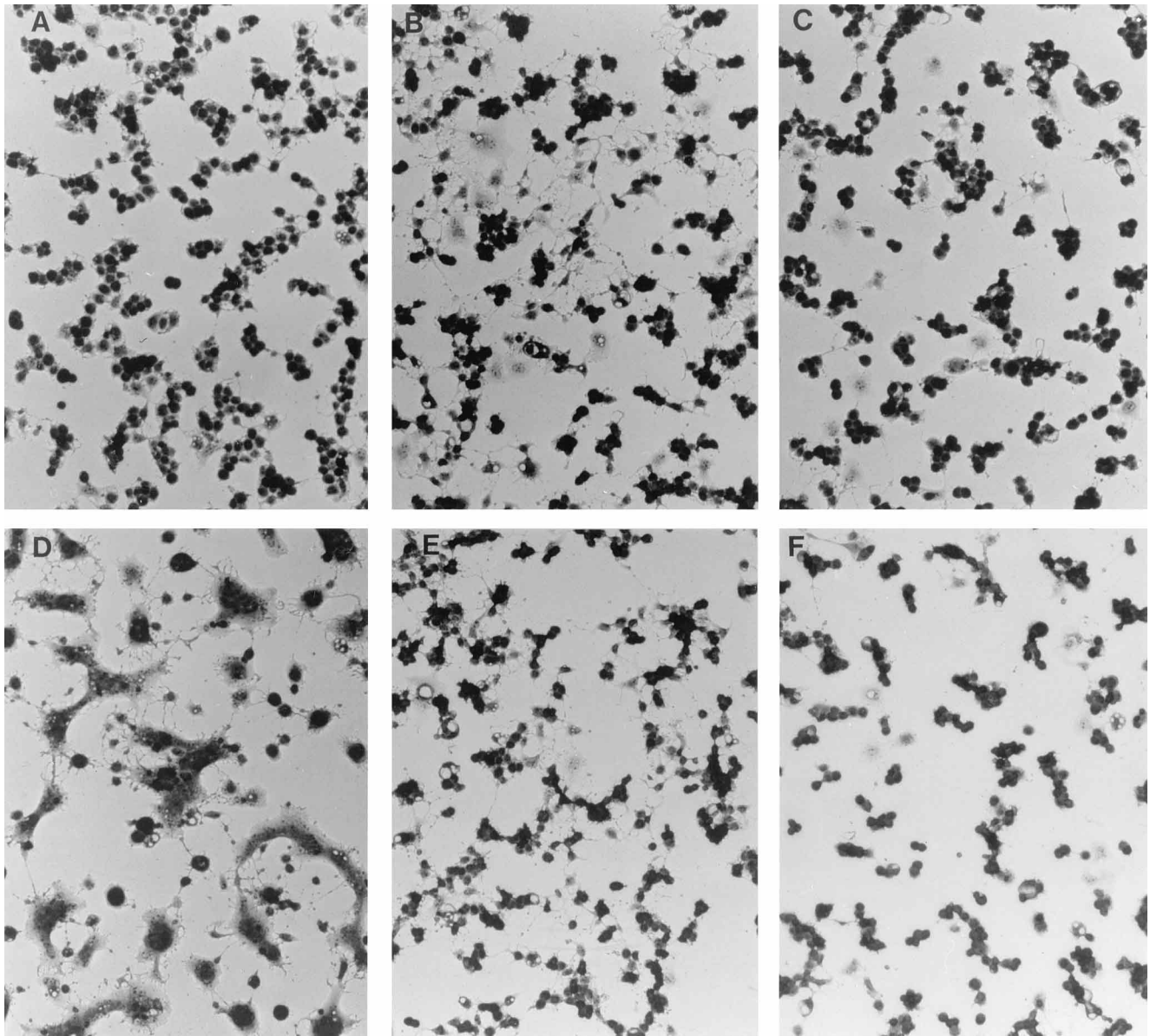
FIG. 7. Vaccinia virus-induced fusion from within. BS-C-1 cells were infected with wild-type vaccinia virus (A and D), vA34R⁻ (B and E), or an F13L deletion mutant (C and F). At 20 h after infection, the cells were briefly exposed to neutral (A to C) or low-pH (D to F) buffer and then incubated for 2.5 h at 37°C in regular medium. The cells were fixed, stained with crystal violet, and photographed through a light microscope.

deletion mutants (Fig. 9G and H, respectively), as well as for WR and IHD-J strains of vaccinia virus (Fig. 9E and F, respectively). In contrast, when the cells were treated with neutral-pH buffer, polykaryon formation did not occur with any of these viruses (Fig. 9A to D). Polykaryon formation also did not occur when uninfected cells were treated with either neutral- or low-pH buffers (data not shown). These studies suggest that neither the A34R protein nor the F13L protein per se is required for fusion, but rather they are required for presentation of the fusion protein on the cell surface.

## DISCUSSION

The small-plaque phenotype of vA34R⁻, an A34R deletion mutant, is similar to that of other vaccinia virus mutants that fail to form extracellular wrapped virions. Although there seems to be some decrease in the number of IEV or IMV undergoing wrapping at any one time (10), our electron microscopic studies revealed that the A34R mutant produced numerous wrapped extracellular particles that were labeled by EEV-specific antibodies and protein A-colloidal gold, consistent with recently reported biochemical studies (26). These data suggest a novel role for the A34R protein in mediating virus spread. McIntosh and Smith (26) presented evidence that the EEV of wild-type vaccinia virus have five- to sixfold greater infectivity than EEV of A34R⁻ virus and that the infectivity of the latter could be increased severalfold by freezing and thawing, which apparently results in the release of infectious IMV. We found additional novel properties of the A34R deletion mutant, namely, defects in induction of actin tails, thickened microvilli, and low-pH-induced fusion, that might contribute to inefficient cell-to-cell spread.
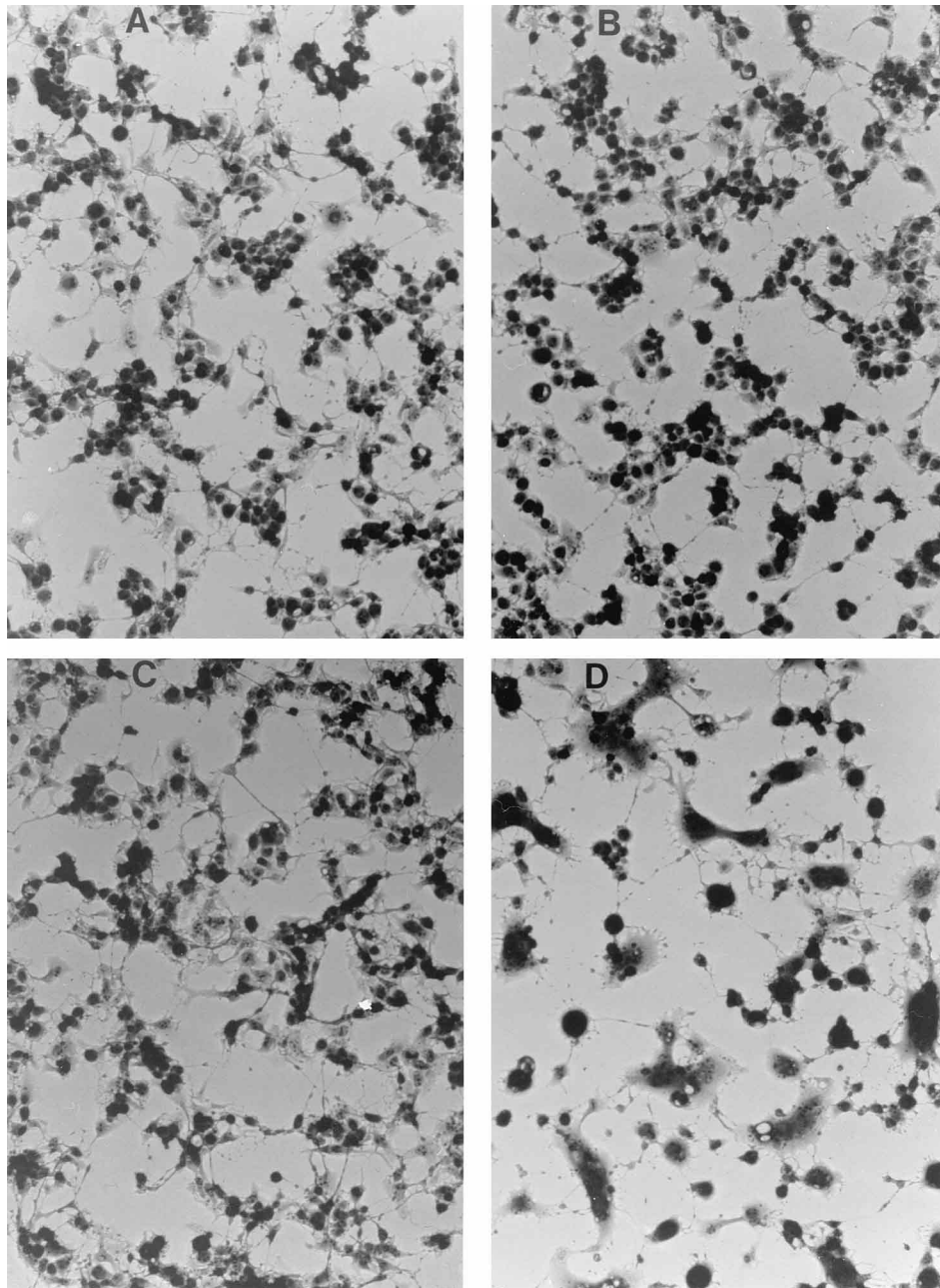
FIG. 8. Induction of fusion from within by IPTG. BS-C-1 cells were infected with vSAD9 in the absence (A and C) or presence (B and D) of IPTG, briefly treated with neutral (A and B) or low-pH (C and D) buffer, and then further incubated with regular medium as described in the legend to Fig. 7.

Previous studies indicated that the induction of actin tails and specialized microvilli correlated with the formation of extracellular vaccinia virions. Thus, rifampin, a drug that inhibits virus assembly at an early stage, prevented actin tail formation (25). Actin tail formation also did not occur when cells were infected with a vaccinia virus mutant that formed IMV but not EEV (3). As shown here, however, actin tails were not seen when expression of the A34R protein was prevented, even though EEV were produced. This result was confirmed by examination of the cell surface by scanning electron microscopy: thick microvilli were abundant on the surfaces of cells infected with wild-type virus but were not detected in the absence of the A34R protein. Even though we obtained similar

results when cells were examined at several different times after infection, it is possible that the actin tails and specialized microvilli formed transiently, perhaps decaying after the A34R mutant virus fused with the plasma membrane. Therefore, it might be useful to examine infected cells by live videomicroscopy (6) instead of by taking snapshot photographs. Despite this caveat, we believe that the data obtained from repeated experiments indicate that there is a defect in the formation of actin-containing specialized microvilli and that this is correlated with the absence of the A34R protein.

Recent data indicate that G actin, not preformed actin filaments, is recruited to IEV particles (7). If the A34R protein has a direct role in actin tail formation, then the short N-
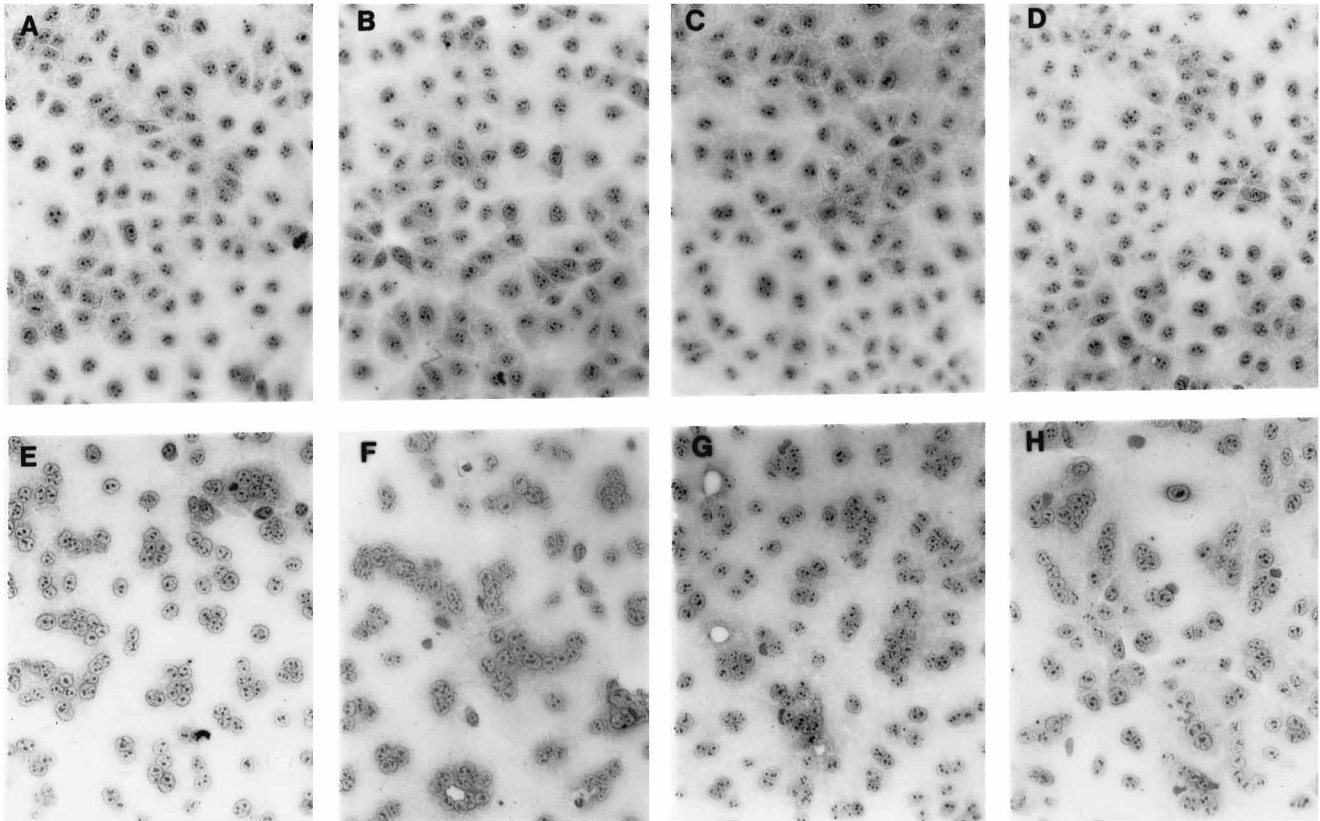
FIG. 9. Vaccinia virus-induced fusion from without. BS-C-1 cells were infected with strain WR vaccinia virus (A and E), strain IHD-J vaccinia virus (B and F), A34R⁻ (C and G), or the F13L deletion mutant (D and H) at a high multiplicity of infection in the presence of cycloheximide for 1.5 h at 0°C. Cells were briefly treated with neutral-pH buffer (A to D) or low-pH buffer (E to H) and then incubated in regular medium at 37°C for 3 h. The cells were fixed, stained, and photographed.

terminal cytoplasmic domain of this putative type II membrane protein might interact with G actin to nucleate or stabilize tail formation. The construction of additional A34R mutant viruses is needed to test this hypothesis. Interestingly, smaller numbers of actin-containing microvilli were noted in cells infected with the IHD-J strain of vaccinia virus than in those infected with the WR strain, but this would have to be attributed to the point-mutational difference in the extracellular lectin homology domain of the A34R protein rather than to a difference in the cytoplasmic domain (4). This mutation might influence actin tail formation by perturbing the A34R protein or its association with other proteins more directly involved in actin tail formation.

Our data suggest that the specialized actin tails are not essential for transporting virions to the cell surface. This interpretation is consistent with the findings of Hiller et al. (20), who had previously noted that the microvilli are not the only sites on the cell periphery with which mature virions are associated. Evidence for other mechanisms of transport and release of enveloped virions has been presented previously (40, 41). The role of actin filaments, not organized into specialized tails, in virus egress was not addressed in our study. However, Payne and Kristensson (31) found numerous EEV on the surfaces of cells infected in the presence of cytochalasin D, which specifically inhibits actin filament polymerization and prevents actin tail formation (6). A distinction between the effects of cytochalasin D and the defect caused by deletion of the A34R gene is that release of EEV was inhibited by the former (31) but not by the latter.

If the actin tails and thickened microvilli are not required for EEV formation and release, what is their function? Cudmore et al. (6) presented immunofluorescence and electron microscopic images of virus-tipped actin projections extending into uninfected cells. Therefore, the principal role of the microvilli may be to facilitate cell-to-cell spread rather than EEV release. A model in which CEV at the tips of the microvilli fuse with the plasma membrane of an adjacent cell (3) is supported by images that show virus particles that appear to be outside the plasma membrane (7, 38). Strauss (39) has argued for a mechanism involving direct cell-to-cell spread of IEV that is more analogous to that used by certain bacteria but which would require the unwrapping of IEV in the recipient cell. Thus, the small-plaque phenotype of A34R⁻ mutants could arise from the absence of protruding virus-tipped microvilli, as suggested here, and/or the low level of infectivity of A34R⁻ EEV reported by McIntosh and Smith (26). The latter workers suggested that the low infectivity level could signify that the A34R protein is required for binding or fusion. An alternative possibility is that the A34R protein is needed for release of IMV from the EEV wrapping membrane during or after the attachment process.

Relatively little work has been done on determining either the mechanism or the significance of low-pH-induced cell-to-cell fusion by vaccinia virus. Gong et al. (15) demonstrated that fusion from without occurred with large numbers of purified intracellular vaccinia virions and was inhibited by antibody to the 14-kDa IMV envelope protein, suggesting that IMV are necessary for this process. However, preparations of purified

intracellular virus usually include some IEV, so the possibility remained that the latter were also needed for fusion. The present study supports the interpretation of Gong et al. because intracellular virus prepared from an F13L deletion mutant, in which IEV formation is totally blocked, induced fusion from without.

Fusion from within is more complicated than fusion from without and has requirements that are similar to those of virus spread. Although Gong et al. (15) provided genetic evidence that the 14-kDa IMV protein was required for fusion from within, others demonstrated that mutants which formed IMV but not EEV because of mutations in the F13R (2) or B5R (42) gene were defective in low-pH-induced fusion from within. Taken together, the data suggested that for fusion to occur, the EEV proteins were required to present virus particles on the cell surface. Here we show that surface presentation is insufficient since A34R⁻ mutants are also defective in low-pH-induced fusion from within. This defect is probably not due to a specific requirement for the A34R protein since A34R-deficient particles could induce fusion from without. Thus, the defect in polykaryon formation could result from the absence of virus-tipped specialized microvilli needed to bridge cells or from altered properties of the extracellular virus.

In conclusion, our studies provide genetic evidence for the involvement of a specific viral protein in the formation or stability of actin-containing microvilli and for a role of these structures in cell-to-cell spread and low-pH-induced fusion from within. Further studies are needed to determine whether the A34R protein acts directly, possibly in conjunction with other EEV proteins, by serving as an actin attachment site or indirectly by altering the kinetics of protein trafficking and membrane-protein interactions.

## ACKNOWLEDGMENTS

## REFERENCES

1. **Blasco, R., N. B. Cole, and B. Moss.** 1991. Sequence analysis, expression, and deletion of a vaccinia virus gene encoding a homolog of profilin, a eukaryotic actin-binding protein. J. Virol. **65:**4598–4608.
2. **Blasco, R., and B. Moss.** 1991. Extracellular vaccinia virus formation and cell-to-cell virus transmission are prevented by deletion of the gene encoding the 37,000-dalton outer envelope protein. J. Virol. **65:**5910–5920.
3. **Blasco, R., and B. Moss.** 1992. Role of cell-associated enveloped vaccinia virus in cell-to-cell spread. J. Virol. **66:**4170–4179.
4. **Blasco, R., J. R. Sisler, and B. Moss.** 1993. Dissociation of progeny vaccinia virus from the cell membrane is regulated by a viral envelope glycoprotein: effect of a point mutation in the lectin homology domain of the A34R gene. J. Virol. **67:**3319–3325.
5. **Brown, C. K., P. C. Turner, and R. W. Moyer.** 1991. Molecular characterization of the vaccinia virus hemagglutinin gene. J. Virol. **65:**3598–3606.
6. **Cudmore, S., P. Cossart, G. Griffiths, and M. Way.** 1995. Actin-based motility of vaccinia virus. Nature **378:**636–638.
7. **Cudmore, S., I. Reckmann, G. Griffiths, and M. Way.** 1996. Vaccinia virus; a model system for actin-membrane interactions. J. Cell Sci. **109:**1739–1747.
8. **Dales, S., and L. Siminovitch.** 1961. The development of vaccinia virus in Earle's L strain cells as examined by electron microscopy. J. Biophys. Biochem. Cytol. **10:**475–503.
9. **Doms, R. W., R. Blumenthal, and B. Moss.** 1990. Fusion of intra- and extracellular forms of vaccinia virus with the cell membrane. J. Virol. **64:**4884–4892.
10. **Duncan, S. A., and G. L. Smith.** 1992. Identification and characterization of an extracellular envelope glycoprotein affecting vaccinia virus egress. J. Virol. **66:**1610–1621.
11. **Earl, P. L., N. Cooper, and B. Moss.** 1991. Preparation of cell cultures and vaccinia virus stocks, vol. 2, p. 16.16.1–16.16.7. In F. M. Ausubel, R. Brent, R. E. Kingston, D. D. Moore, J. G. Seidman, J. A. Smith, and K. Struhl (ed.), Current protocols in molecular biology. Greene Publishing Associates & Wiley Interscience, New York, N.Y.
12. **Earl, P. L., and B. Moss.** 1991. Generation of recombinant vaccinia viruses, vol. 2, p. 16.17.1–16.17.16. In F. M. Ausubel, R. Brent, R. E. Kingston, D. D. Moore, J. G. Seidman, J. A. Smith, and K. Struhl (ed.), Current protocols in molecular biology. Greene Publishing Associates & Wiley Interscience, New York, N.Y.
13. **Engelstad, M., S. T. Howard, and G. L. Smith.** 1992. A constitutively expressed vaccinia gene encodes a 42-kDa glycoprotein related to complement control factors that forms part of the extracellular virus envelope. Virology **188:**801–810.
14. **Engelstad, M., and G. L. Smith.** 1993. The vaccinia virus 42-kDa envelope protein is required for the envelopment and egress of extracellular virus and for virus virulence. Virology **194:**627–637.
15. **Gong, S. C., C. F. Lai, and M. Esteban.** 1990. Vaccinia virus induces cell fusion at acid pH and this activity is mediated by the N-terminus of the 14-kDa virus envelope protein. Virology **178:**81–91.
16. **Hiller, G., H. Eibl, and K. Weber.** 1981. Characterization of intracellular and extracellular vaccinia virus variants: $N_1$-isonicotinoyl-$N_2$-3-methyl-4-chlorobenzoylhydrazine interferes with cytoplasmic virus dissemination and release. J. Virol. **39:**903–913.
17. **Hiller, G., C. Jungwirth, and K. Weber.** 1981. Fluorescence microscopical analysis of the life cycle of vaccinia virus in chick embryo fibroblasts. Virus-cytoskeleton interactions. Exp. Cell Res. **132:**81–87.
18. **Hiller, G., and K. Weber.** 1982. A phosphorylated basic vaccinia virion polypeptide of molecular weight 11,000 is exposed on the surface of mature particles and interacts with actin-containing cytoskeletal elements. J. Virol. **44:**647–657.
19. **Hiller, G., and K. Weber.** 1985. Golgi-derived membranes that contain an acylated viral polypeptide are used for vaccinia virus envelopment. J. Virol. **55:**651–659.
20. **Hiller, G., K. Weber, L. Schneider, C. Parajsz, and C. Jungwirth.** 1979. Interaction of assembled progeny pox viruses with the cellular cytoskeleton. Virology **98:**142–153.
21. **Hirt, P., G. Hiller, and R. Wittek.** 1986. Localization and fine structure of a vaccinia virus gene encoding an envelope antigen. J. Virol. **58:**757–764.
22. **Isaacs, S. N., E. J. Wolffe, L. G. Payne, and B. Moss.** 1992. Characterization of a vaccinia virus-encoded 42-kilodalton class I membrane glycoprotein component of the extracellular virus envelope. J. Virol. **66:**7217–7224.
23. **Katz, E., E. J. Wolffe, and B. Moss.** 1997. The cytoplasmic and transmembrane domains of the vaccinia virus B5R protein target a chimeric human immunodeficiency virus type 1 glycoprotein to the outer envelope of nascent vaccinia virions. J. Virol. **71:**3178–3187.
24. **Kohno, K., J. Sambrook, and M.-J. Gething.** 1988. Effect of lysosomatotropic agents on the entry of vaccinia virus into CV-1 cells. J. Cell. Biochem. Suppl. **12:**29.
25. **Krempien, U., L. Schneider, G. Hiller, K. Weber, E. Katz, and C. Jungwirth.** 1981. Conditions for pox virus-specific microvilli formation studied during synchronized virus assembly. Virology **113:**556–564.
26. **McIntosh, A. A. G., and G. L. Smith.** 1996. Vaccinia virus glycoprotein A34R is required for infectivity of extracellular enveloped virus. J. Virol. **70:**272–281.
27. **Morgan, C.** 1976. Vaccinia virus reexamined: development and release. Virology **73:**43–58.
28. **Parkinson, J. E., and G. L. Smith.** 1994. Vaccinia virus gene A36R encodes a Mr 43-50 K protein on the surface of extracellular enveloped virus. Virology **204:**376–390.
29. **Payne, L.** 1978. Polypeptide composition of extracellular enveloped vaccinia virus. J. Virol. **27:**28–37.
30. **Payne, L. G.** 1992. Characterization of vaccinia virus glycoproteins by monoclonal antibody preparations. Virology **187:**251–260.
31. **Payne, L. G., and K. Kristensson.** 1982. The effect of cytochalasin D and monensin on enveloped vaccinia virus release. Arch. Virol. **74:**11–20.
32. **Reckmann, I., S. Higley, and M. Way.** Personal communication.
33. **Roper, R. L., L. G. Payne, and B. Moss.** 1996. Extracellular vaccinia virus envelope glycoprotein encoded by the A33R gene. J. Virol. **70:**3753–3762.
34. **Schmutz, C., L. Rindisbacher, M. C. Galmiche, and R. Wittek.** 1995. Biochemical analysis of the major vaccinia virus envelope antigen. Virology **213:**19–27.
35. **Seki, M., M. Oie, Y. Ichihashi, and H. Shida.** 1990. Hemadsorption and fusion inhibition activities of hemagglutinin analyzed by vaccinia virus mutants. Virology **175:**372–384.
36. **Shida, H.** 1986. Nucleotide sequence of the vaccinia virus hemagglutinin gene. Virology **150:**451–462.
37. **Sodeik, B., R. W. Doms, M. Ericsson, G. Hiller, C. E. Machamer, C. van't Hof, G. van Meer, B. Moss, and G. Griffiths.** 1993. Assembly of vaccinia virus: role of the intermediate compartment between the endoplasmic reticulum and the Golgi stacks. J. Cell Biol. **121:**521–541.
38. **Stokes, G. V.** 1976. High-voltage electron microscope study of the release of vaccinia virus from whole cells. J. Virol. **18:**636–643.
39. **Strauss, E. J.** 1996. Intracellular pathogens: a virus joins the movement. Curr. Biol. **6:**504–507.
40. **Tsutsui, K.** 1983. Release of vaccinia virus from FL cells infected with the

IHD-W strain. J. Electron Microsc. **32:**125–140.

41. **Tsutsui, K., F. Uno, K. Akatsuka, and S. Nii.** 1983. Electron microscopic study on vaccinia virus release. Arch. Virol. **75:**213–218.

42. **Wolffe, E. J., S. N. Isaacs, and B. Moss.** 1993. Deletion of the vaccinia virus B5R gene encoding a 42-kilodalton membrane glycoprotein inhibits extracellular virus envelope formation and dissemination. J. Virol. **67:**4732–4741.

43. **Wolffe, E. J., D. M. Moore, P. J. Peters, and B. Moss.** 1996. Vaccinia virus A17L open reading frame encodes an essential component of nascent viral membranes that is required to initiate morphogenesis. J. Virol. **70:**2797–2808.

44. **Wolffe, E. J., S. Vijaya, and B. Moss.** 1995. A myristylated membrane protein encoded by the vaccinia virus L1R open reading frame is the target of potent neutralizing monoclonal antibodies. Virology **211:**53–63.

45. **Zhang, Y., and B. Moss.** 1991. Vaccinia virus morphogenesis is interrupted when expression of the gene encoding an 11-kilodalton phosphorylated protein is prevented by the *Escherichia coli lac* repressor. J. Virol. **65:**6101–6110.